Research Article OPEN ACCESS

Volume-10 | Issue-2 | Apr-Jun - 2024|

Check for updates

VEETHIKA-An International Interdisciplinary Research Journal
E-ISSN: **2454-342x**
Peer Reviewed
URL: https://veethika.qtanalytics.in

Utilizing Geological and Geoelectrical methods in a GIS-based DRASTIC model of the Probable Groundwater Vulnerability in the Southern Nigerian Raffia Metropolis of Ikot Ekpene and its Surroundings

Emem O. IKPE[1*], Udeme U. INYANG[2], Itoro A. SAMPSON[3]

Department of Science Technology, School of Applied Sciences, Akwa Ibom State Polytechnic, Ikot Osurua, Akwa Ibom State, Nigeria

**Corresponding Author* Email: emem.ikpe@akwaibompoly.edu.ng

Orcid Id: 0000-0001-8093-9904[1], 0009-0009-4461-1704[2], 0009-0006-1890-6160[3]

Received: 10 April 2024, ***Revised:*** 1 May 2024, ***Accepted:*** 14 May 2024, ***Published***: 19 May 2024

ABSTRACT: Ikot Ekpene is experiencing a pressing challenge with groundwater contamination due to the increasing amount of home and industrial waste. This is as a result of the increasing human population and various business operations in the area producing more residential and industrial waste. This study aims to assess the vulnerability of groundwater in the metropolis of Ikot Ekpene and its environs in southern Nigeria by utilizing geological and geoelectrical methods within a GIS-based DRASTIC model. It will utilize integrated geoelectrical and geological approaches within the GIS-based DRASTIC model. A total of twenty vertical electrical soundings (VES) were conducted in the region using the Schlumberger array. Based on the geological drilling data, the interpretation of the VES data suggests that the area consists of 3–4 geoelectric layers. The lithological succession in the region displays a variety of sediment types, such as fine sand, coarse sand, and gravelly sands, along with localized occurrences of clay intercalations. Additionally, there are localized occurrences of clay intercalations. The third geoelectric layer, located at a depth of 9.0–86.6 m, is the primary aquifer that can be utilized in the region. The DRASTIC model included seven environmental parameters, including depth to the water table, net recharge, aquifer medium, topography, impact of the vadose zone, and hydraulic conductivity, with the purpose of conducting a vulnerability assessment. The assessment of groundwater vulnerability ratings (GVR) reveals that 75% of the research region is classified as high vulnerability, 20% as moderate vulnerability, and the remaining 5% as low vulnerability. The studied area is predominantly characterized by a moderate to high groundwater vulnerability rating (GVR), which is likely attributed to the generally gentle topography and the presence of highly permeable geomaterials in the upper levels of the water table.

KEYWORDS: DRASTIC, GIS, Aquifer media, Permeability, Groundwater, Topography

DOI: https://doi.org/10.48001/veethika.2024.10.02.003

1. INTRODUCTION:

Groundwater is becoming more desirable as a supply of drinkable water for the growing global population. This is mainly due to its abundance and, more importantly, its higher quality compared to surface water sources like streams, lakes, and rivers. Groundwater is held beneath the Earth's surface in geological formations called aquifers, which are not perceptible to the human eye. These aquifers are vulnerable to pollution or contamination from either natural or human activities (Ekanem, 2022; Ekanem et al., 2022; Kumar & Krishna, 2020; Machiwal et al., 2018). These operations result in the contamination of groundwater, rendering it unsuitable for human use. Groundwater contamination has emerged as a significant global concern because to its substantial effects on human health and ecological services (Ekanem, 2022; George, 2021; Ikpe et al., 2022; Li et al., 2021). As a result, the assessment of groundwater vulnerability has become a useful method for identifying areas that are susceptible to contamination. This is done in order to develop effective strategies for managing and protecting groundwater (Ekanem, 2022; Ikpe et al., 2022; Kumar & Krishna, 2020). Groundwater vulnerability potential is the measure of the level of natural protection provided by the environment to prevent the spread of contaminants in groundwater.

The geological characteristics of a region determine the duration it takes for surface contaminated water, such as precipitation, to filter through the soil and reach the water table (Ekanem, 2020; George, 2021). Surface contaminants or pollutants can seep into the groundwater and cause contamination, depending on the characteristics of the geological materials located above the water table. In this case, "vulnerability" refers to how easy it is for surface or near-surface pollutants to get into underground hydrogeological formations and pollute or contaminate groundwater (Foster et al., 2013; Harter & Walker, 2001). The time it takes for pollutants to reach the water table has a significant impact on the level of pollution (Maxe & Johansson, 1998). This duration is determined by factors such as the depth of the water table, the properties of the vadose zone, net recharge, and the chemical properties of the pollutants (Abu-Bakr, 2020; Kumar & Krishna, 2020). Deeper aquifers are less vulnerable to pollutants compared to shallow ones. Groundwater vulnerability can be categorized into two types: intrinsic (natural) vulnerability and particular (integrated) vulnerability (NRC, 1993; Vrba and Zoporozec, 1994). Intrinsic vulnerability, also known as natural vulnerability, refers to the susceptibility of an area to the infiltration and diffusion of surface-originated contaminants into the water table and groundwater. This vulnerability is determined by the geological, hydrological, and hydrogeological characteristics of the area. Specific vulnerability refers to the contamination of groundwater caused by a specific contaminant or group of contaminants. It is determined by the properties of the contaminants, including the duration and strength of their impact, as well as the interaction between the intrinsic vulnerability components and the contaminant in question (Doerfliger et al., 1999; Gogu & Dassargues, 2000a).

There are multiple techniques that can be used to conduct groundwater vulnerability assessments. The approaches mentioned are the DRASTIC method (Aller et al., 1987), GOD method (Foster, 1987), AVI method (Van Stempvoort et al., 1992), SIN-TACS method (Civita, 1990), and SI method (Boufekane & Saighi, 2013). The DRASTIC method is widely favoured due to its simplicity, accessibility of essential data, and clear elucidation of groundwater vulnerability (Awawdeh & Jaradat, 2010; Neh et al., 2014; Awawdeh et al., 2015; Barbulescu, 2020). This method employs seven characteristics for vulnerability assessment (Aller et al., 1987). The parameters that comprise the acronym 'DRASTIC' are depth to groundwater (D), net recharge (R), aquifer media (A), soil media (S), topography (T), impact of the vadose zone (I), and aquifer hydraulic conductivity (C). The presence of these input parameters plays a crucial role in reducing the influence of inaccuracies in individual factors on the ultimate outcomes, thereby enhancing the model's effectiveness in evaluating groundwater risk. A significant limitation of the DRASTIC model is the inherent subjectivity involved in assigning weights and ratings to the various parameter components of the model (Gogu & Das-Sargues, 2000b; Chitsazan and Akhtari, 2008). Nevertheless, the model has proven to be effective in evaluating the susceptibility of groundwater in various regions across the globe (Abdullahi, 2009; Abu-Bakr, 2020; Amiri et al., 2020; Awawdeh & Jaradat, 2010; Awawdeh et al., 2015; Barbulescu, 2020; George, 2021; Kumar & Krishna, 2020; Shirazi et al., 2013; Ven- katesan et al., 2019).

This research employed the DRASTIC model to assess the vulnerability of groundwater in the raffia metropolis of Ikot Ekpene and its neighbouring regions in southern Nigeria, integrating geological and geoelectrical methods within the model. The input parameters for the DRASTIC model were derived from the VES data interpretation findings, with the exception of topography, which was computed using the ASTER digital elevation model (DEM) in ArcGIS 10.5. The VES approach is a valuable tool for studying the patterns of electrical resistivity variation in the subsurface. It is a fast and cost-effective

DOI: https://doi.org/10.48001/veethika.2024.10.02.003

method for imaging underground aquifers. This has been demonstrated by studies conducted by Ekanem et al. (2020), George (2021), Ikpe et al. (2022), and Udoh et al. (2015). Compared to traditional well drilling methods, the VES methodology is more cost-effective and environmentally friendly. This is because it only relies on surface measurements and does not include the actual digging of boreholes (Ekanem et al., 2020; George et al., 2018; Udoh et al., 2015). Ikot Ekpene has faced water scarcity issues due to population growth and urbanization, exacerbated by the lack of sufficient surface water bodies in the area (George et al., 2016a, 2017; Ikpe et al., 2022). The population of Ikot Ekpene municipality and its surrounding areas have relied heavily on groundwater as a geo-resource to meet their growing water demands. The escalating human population, in conjunction with other business activity in the region, leads to a proportional rise in both home and industrial trash in the area. The municipality of Ikot Ekpene is facing a significant challenge with indiscriminate waste disposal. The streets in the area are filled with heaps of various types of solid waste, including domestic waste, vegetable waste, waste paper, scrap metal, chemical-filled cans, plastic containers, old rags, vehicle tires, scalpels, and human waste. This issue has been documented by Ikpe et al. (2022) and Umoh and Etim (2013). During precipitation, certain perilous substances infiltrate the hydrogeological formations in the vicinity, leading to the pollution of groundwater. This contamination presents significant threats to human well-being and the overall ecological balance. George et al. (2014) utilized geophysical, geochemical, and hydrogeological data to evaluate the impact of leachates on the quality of groundwater in the vicinity of the former dumpsite in the research region. Their findings indicated that the impact of leachates was more significant in the identified groundwater reservoirs located near the dumpsite compared to those located further away. In this work, Ikpe et al. (2022) employed the VES and electrical resistivity tomography (ERT) methods to evaluate the protective capacity of hydrogeological units in the studied area. The evaluation results indicate that 75% of the study region has a low protectivity rating, 20% has a moderate rating, and only 5% has a high rating. These data suggest that the uppermost layers of the study region are highly susceptible to contamination on the surface or just below it. Consequently, this study was essential for identifying the areas with a high susceptibility to harm in order to facilitate the creation of an effective plan for developing and exploring groundwater, as well as implementing a suitable waste disposal system in the area by the relevant authorities.

1.1 Description of the Study Area

The research was carried out in the metropolis of Ikot Ekpene and the surrounding areas in southern Nigeria (Fig. 1). The region is situated within the latitudes of 5.072°–5.140° N and longitudes of 7.390°–7.458° E, with a total area of approximately 119 km^2. In the area, the highest point above the average sea level is 102 meters in the northern portion, while the lowest point is 54 meters in the southern part. The city can be reached through an extensive road network and is a prominent center for business activities in Akwa Ibom State, located in southern Nigeria. The region is encompassed by the inland coastal water and characterized by rainforest flora. The mean annual precipitation in the region is approximately 2007.9 millimetres (Isaiah et al., 2021).

Ikot Ekpene is located in a region with a humid tropical environment, which is its climatic characteristic. Over the course of two seasons. The seasons consist of the dry season, which occurs from November to April, and the rainy or wet season, which occurs from March to October. The dominant wind pattern in the region during the dry season is the Harmattan winds originating from the north, while the monsoon winds from the Atlantic Ocean prevail during the rainy season (Vrbka et al., 1999). The research area experiences a variation in annual temperatures, ranging from 20 °C during the wet or rainy season to around 35 °C during the dry season (Ekanem, 2020; George et al., 2017, 2021).

Geologically, Ikot Ekpene is located in the Niger Delta province, immediately on the Gulf of Guinea in the Atlantic Ocean, in the southern region of Nigeria. The province is partitioned into three primary stratigraphic units: the Benin Formation, the Agbada Formation, and the Akata Formation, located at the base of the Delta. These formations are depicted in the schematic diagram shown in Figure 2, as referenced by Obaje (2009), Short and Stauble (1967), and Stacher (1995). The Benin Formation is the most recent and uppermost section of the Niger Delta. It consists of coastal plain sands (CPS) that vary in size from fine to coarse, as well as gravels (Mbipom et al., 1996; Short & Stauble, 1967). Groundwater extraction in the city of Ikot Ekpene is carried out in the coastal plains of the Benin Formation. This area is known for having layers of clay, silt, and sandstones in various areas (Reijers and Petters, 1987). In certain areas of the research site, a multi-aquifer system is formed by the alternating layers of sand and clay (Edet & Okereke, 2002; Esu et al., 1999).

DOI: https://doi.org/10.48001/veethika.2024.10.02.003

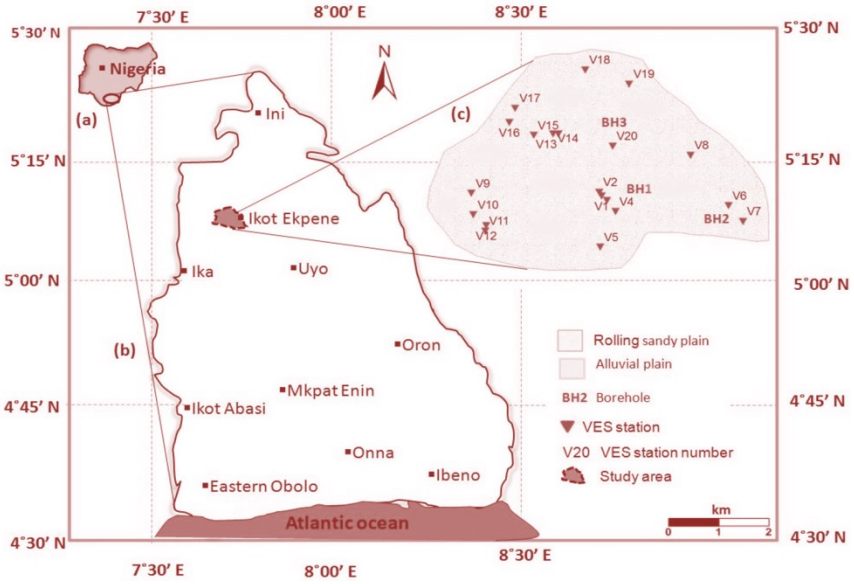

Figure 1: Map of **a** Nigeria showing Akwa Ibom State in southern Nigeria. **b** Akwa Ibom State showing the study area, **c** study area showings its geology and sounding stations

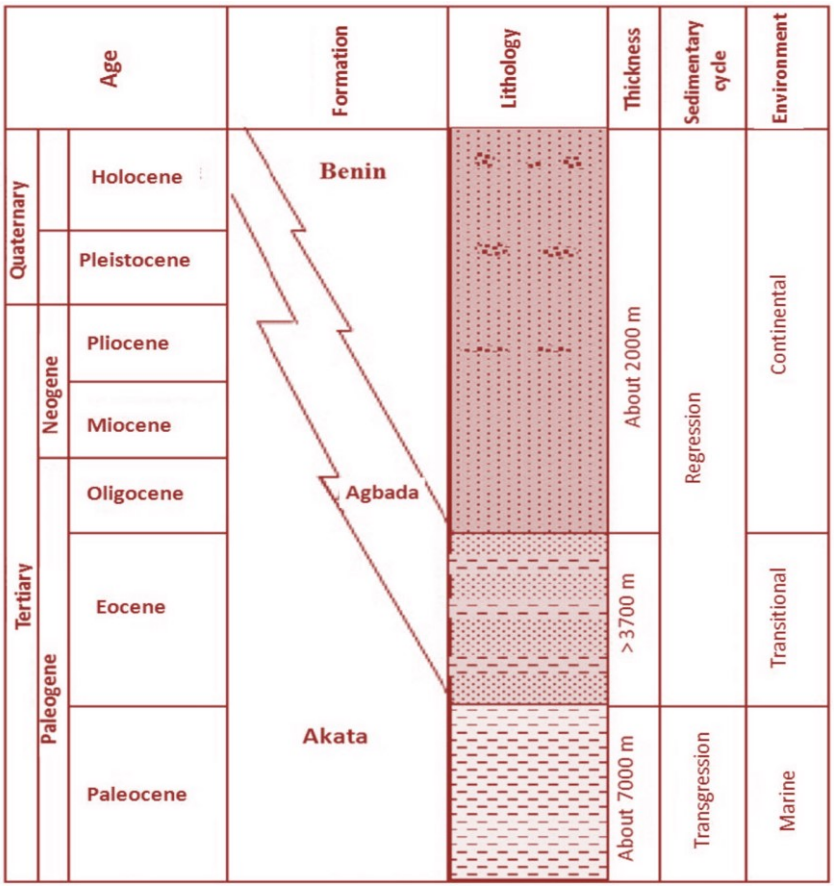

Figure 2: A schematic diagram showing the general Stratigraphy of the Niger Delta, where the study area is located (adapted from Obaje, 2009)

DOI: https://doi.org/10.48001/veethika.2024.10.02.003

2. MATERIALS AND METHOD

This study used two sets of data in combination with the GIS-based DRASTIC model to evaluate the susceptibility of groundwater in the city of Ikot Ekpene and its surrounding areas. The files consist of geophysical data obtained by the electrical resistivity technique and borehole geological data. The electrical resistivity approach employed the Schlumberger electrode design to conduct vertical electrical soundings (VES) in the subject region. The obtained resistivity data were analysed using the WINRESIST software tool to determine the primary geoelectric parameters of the layers through which the electric current passed. The qualities in question are resistivity, thickness, and depth. The lithological logs obtained from drilled boreholes in the research area were utilized as benchmarks for identifying the different lithological and hydrogeological units based on the interpreted resistivity data.

2.1 VES data acquisition, analysis and interpretation

The IGIS signal enhancement resistivity meter SSP-MP-ATS, together with its attachments, was utilized to conduct a one-dimensional (1D) electrical resistivity sounding in several locations within the raffia city of Ikot Ekpene and its surrounding areas, as depicted in Figure 1. The electrode configuration developed by Schlumberger was used in the field survey, as described in the studies by Bello et al. (2010), Udoh et al. (2015), George et al. (2014, 2017, 2018, 2021), Thomas et al. (2020), Ekanem et al. (2021), and others. This configuration consists of two current electrodes, A and B, which are utilized to introduce a precisely defined electric current into the subsurface. Additionally, there are two potential electrodes, M and N, which are employed to measure the resulting potential difference. Four electrodes were positioned in a linear arrangement on the surface of the Earth. The resistivity meter provided the measured resistance of the earth layers, which was presented on its liquid crystal display (LCD) in ohms (Ω). The distance between the electrodes, AB, was systematically raised around the center of the measurement to allow for deeper current penetration. Additionally, the distance between the potential electrodes, MN, was periodically increased. These procedures were described in studies by Ekanem et al. (2020), George et al. (2018, 2020), and Thomas et al. (2020). The highest value recorded for AB in this investigation was 400 meters, while the highest value for MN was 20 meters. At all the occupied sounding stations, the spacing between the electrodes was carefully set to ensure that AB/2 ≥ 5 MN/2, in accordance with the assumption of potential gradient (Dobrin & Savit, 1988). Three soundings were conducted at three water boreholes in the vicinity, as indicated in Figure 1. The lithological logs from the boreholes were utilized to limit the interpretation of the VES data during the computer modelling phase. The logs were utilized to restrict the starting layer thicknesses and depths throughout the modelling phase and also assisted in identifying the different lithological and hydrogeological units in the area based on the final modelling curves. Initially, the raw apparent resistance (Ra) obtained from field measurements was transformed into apparent resistivity ρa using Equation (1):

$$\rho_a = \pi \times \left\{ \frac{\left(\frac{AB}{2}\right)^2 - \left(\frac{MN}{2}\right)^2}{MN} \right\} \times R_a \qquad (1)$$

The apparent resistivity values obtained for each VES location were plotted against half of the current electrode separations (AB/2) on a bi-logarithmic scale to generate the VES sounding curves. The curves were manually smoothed to eliminate any erroneous patterns, which is likely to result in elevated root mean square errors during the computer-aided stage of the data interpretation The changes in the obtained smoothed curves were solely related to the vertical resistivity distribution in the subsoil. The initial thicknesses and resistivities of the layers were determined by performing partial curve matching on the smoothed curves (Zohdy et al., 1974). The initial parameters were utilized as inputs in the computer-aided interpretation conducted with the assistance of the WIN-RESIST computer software application, with the borehole lithological logs serving as controls. The computer software utilizes the initial layer parameters to create a theoretical model and then compares it with the field data to generate the final VES curves. The quality of the match is determined by the root mean square errors. The ultimate 1D resistivity model curves enable the precise determination of the true thickness, resistivity, and depth of the different litho units. Figure 3 displays examples of the final VES curves and their relationships with the existing lithological logs. The VES interpretations show a relatively strong correlation with the borehole lithological logs, despite some discrepancies in the inferred depths of the layers compared to the depths recorded in the logs. This is feasible since there might not be a complete alignment between the geological section and the geoelectric sections (Bello et al., 2010).

2.2 DRASTIC model for groundwater vulnerability assessment

DOI: https://doi.org/10.48001/veethika.2024.10.02.003

DRASTIC is an abbreviation that stands for Depth (D), Net Recharge (R), Aquifer Media (A), Soil Media (S), Topography (T), Impact of the Vadose Zone (I), and Hydraulic Conductivity of the Aquifer (C). The DRASTIC model is formed by combining these seven parameters. The DRASTIC model, designed by the US Environmental Protection Agency (Aller et al., 1987; US EPA, 1994), is a frequently utilized model for assessing groundwater vulnerability (Awawdeh & Jaradat, 2010; Bar-Bulescu, 2020). Each of the seven characteristics is assigned a weight (W) ranging from 1 to 5, based on its level of severity in relation to groundwater vulnerability (Aller et al., 1987). The most severe parameters are awarded a weight of 5, while the least severe ones are allocated a weight of 1. The weights assigned to the parameters, as reported by Aller et al. (1987) and Barres-Lallemend (1994), can be found in Table 1.

$$\text{DRASTIC INDEX} = D_rD_w + R_rR_w + A_rA_w + S_rS_w + T_rT_w + I_rI_w + C_rC_w \quad (2)$$

Table 2 presents the modified classification of Aller et al. (1987) and Amiri et al. (2020) that is used to rate the groundwater vulnerability using the index. The potential for groundwater vulnerability increases with a higher DRASTIC score and vice versa.

3. RESULTS AND DISCUSSION

Three to four geoelectric strata with matching resistivities, thicknesses, and depths are revealed by the VES data interpretation, as shown in Table 3. The resistivity distribution pattern, which was limited by the geological drilling lithological data from the accessible boreholes in the region, was used to evaluate the lithology of the geoelectric layers.

The topmost layer (layer 1), whose resistivity values range from 157.3 to 1278.2 Ωm and 0.6–19.2 m in thickness. In addition to the continuous bioturbating activities in the layer, the deceptive character of the layer may be the cause of the significant variabilities in resistivity seen in this motley topsoil (Ekanem et al., 2021; George et al., 2016a). The second layer, whose resistivity values range from 31.8 to 2648.10 Ωm and thickness from 7.6 to 80.9 m, lies beneath the motley topsoil. In certain places, this layer was understood to be sandy clay, and in other places, it was thought to be fine-graded sand. The layer's large variability in resistivity could perhaps be attributed to the layer's geomaterials' variable grain sizes, which are characteristic of the Niger Delta province's Coastal Plain sands (Ekanem, 2021; Mbipom et al., 1996). The resistivity range of the third layer, which is found between 9.0 and 86.6 m below the surface, is 214.4 to 2839.0 Ωm. This layer represents the main exploitable hydrogeological units (aquifers) in the research region, according to the resistivity variation pattern and data from the local borehole lithological logs that are currently accessible. According to the constraints of the borehole lithological logs, the layer was interpreted as fine/coarse sands/sandy clay at some areas and gravelly sands at other locations. As a result, a wide range of resistivity variation was detected in the layer. Table 4 provides an overview of the aquifer's characteristics. Because the aquifers lack confining impermeable layers, they are typically unconfined. The fourth and final geoelectric layer, which exhibits resistivity values ranging from 45.0 to 865.4 Ωm, was identified and interpreted as fine sands at certain areas (VESs 1, 4, 5, 8, 18, and 20) and sandy clay at other locations (VESs 11, 12, and 17). The thickness and depth of this final layer could not be determined because the maximum current electrode spacing of 400 m prevented the injected current from penetrating to the bottom of the layer. These interpretations in the research region are comparable to those of George et al. (2014) and Ikpe et al. (2022). The resistivity results in this study could be affected by the following factors: salinity, water content, clay content, density, form, size, pore size and porosity, and lithology.

DOI: https://doi.org/10.48001/veethika.2024.10.02.003

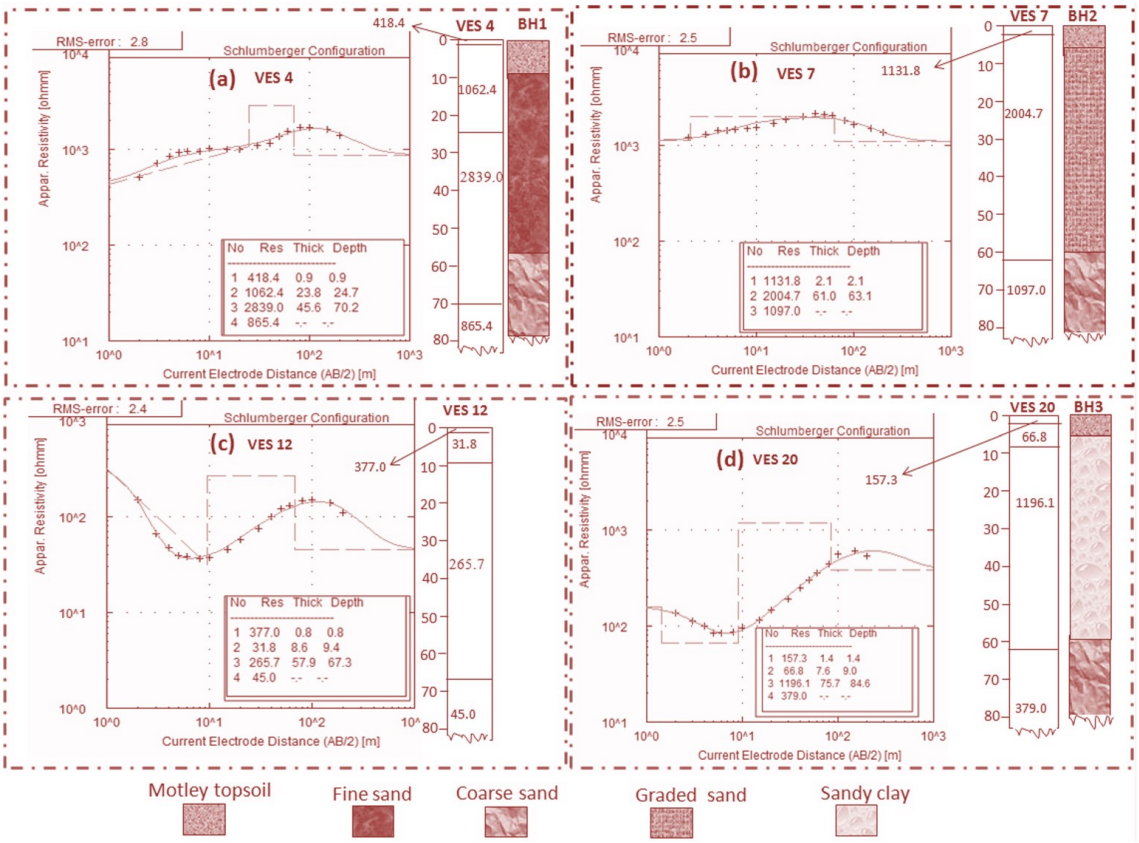

Figure 3: Sample interpreted VES curves **a** VES 4—Utu Ikpe, **b** VES 7—Utu Uyo Road, **c** VES 12—AKWAPOLY, **d** VES 20 Library Avenue. The inserted legends show correlations of borehole lithological logs with the VES results at VESs 4, 7 and 20. The results of VES interpretations correlate fairly well with the borehole lithological logs

3.1 Result of groundwater vulnerability assessment

Table 1: Ranges, ratings and weight of DRASTIC factor

Depth of water (m)			Aquifer media			Soil media			Topography			Impact of vadose zone			Hydraulic conductivity (m/s)		
Interval	R	W	Interval	R	W	Interval	R	W	Interval	R	W	Interval	R	W	Interval	R	W
<20	10	5	Massive shale	2	3	Thin or absent	10	2	0-5	10	1	Thin or absent	10	5	$>9.4\times10^{-4}$	10	
20-40	9		Metamorphic/Igneous	3		Gravel	10					Gravel	10		$4.7\times10^{-4}-9.4\times10^{-4}$	8	
40-60	7		Weathered	4		Sand	9		5-15	8		Sand	9		$32.9\times10^{-5}-4.7\times10^{-4}$	6	
60-80	5		Glacial Tile	5		Laterite/peat	8					Laterite/peat	8		$14.7\times10^{-4}-32.9\times10^{-5}$	4	
80-100	3		Bedded Sandstones	6		Shrinking and/aggregated clay	7		15-25	6		Shrinking and/aggregated clay	7		$4.7\times10^{-5}-14.7\times10^{-5}$	2	
100-120	2		Limestone and Shale			Sandy Loam	6					Sandy Loam	6				
>120	1		Sequences	6		Loam	5		25-35	4		Loam	5		$4.7\times10^{-7}-4.7\times10^{-5}$	1	
			Massive Sandstone	6		Silty Loam	4					Silty Loam	4				
			Massive Limestone	6		Clay Loam	3		>35	1		Clay Loam	3				
			Sand and Gravel	8		Muck	2					Muck	2				
			Basalt	9		Nonshrinky and aggregated clay	1					Nonshrinky and aggregated clay	1				
			Karst Limestone	10													

DOI: https://doi.org/10.48001/veethika.2024.10.02.003

Table 2: DRASTIC Index and Vulnerability Class

DRASTIC Index (DI)	Vulnerability Class
1 – 100	Low
101 – 175	Moderate
176 – 200	High
>200	Very high

Table 3: Summary of VES data interpretation results

VES No	Location	Longitude (Degrees)	Latitude (Degrees)	No. of Layers	Resistivity (Ωm)	Thickness (m)	Depth (m)	Lithology
1	Dumpsite 1 - Utu Ikpe	7.7038	5.1644	4	1190.2 248.6 1750.8 418.7	2.6 8.5 49.2	2.6 11.1 60.3	Coarse sand Sandy sand Gravelly sand Fine sand
2	Dumpsite 2- Utu Ikpe	7.7031	5.1656	3	1278.2 639.4 1621.6	5.6 56.7	5.6 62.3	Coarse sand Fine sand Gravelly sand
3	Utu Ikpe near Prison	7.7053	5.1631	3	430.7 2283.3 851.2	1.1 60.4	1.1 61.5	Fine sand Gravelly sand Coarse sand
4	Utu Ikpe near Palace	7.7078	5.1598	4	418.4 1062.4 2839.0 865.4	0.9 23.8 45.6	0.9 24.7 70.3	Coarse sand Coarse sand Gravelly sand Fine sand
5	Abiakpo Edem Idim	7.7033	5.1491	4	1028.8 339.2 2129.4 760.3	0.6 10.4 54.0	0.6 11.0 65.0	Coarse sand Sandy clay Gravelly sand Fine sand
6	Ibiakpan Nto Akan	7.7400	5.1615	3	193.5 831.7 1341.6	1.6 64.4	1.6 66.0	Sandy clay Fine sand Coarse sand
7	Utu Uyo Road	7.7442	5.1568	3	1131.8 2004.7 1097.0	2.1 61.0	2.1 63.1	Coarse sand Gravelly sand Coarse sand
8	Ikpon Road	7.7292	5.1767	4	590.7 149.2 2478.6 827.9	1.3 11.1 61.4	1.3 12.4 73.8	Fine sand Clay Gravelly sand Fine sand
9	Abiakpo Ntak Inyang	7.6667	5.1652	3	487.8 1021.5 2632.2	2.1 53.5	2.1 55.6	Fine sand Coarse sand Gravelly sand
10	Akwa Poly P1	7.6672	5.1588	3	334.0 89.6 214.4	19.2 67.4	19.2 86.6	Sandy clay Clay Sandy clay
11	Akwa Poly P2	7.6706	5.1539	4	590.8 72.1 722.9 83.3	5.5 16.7 45.2	5.5 22.2 67.4	Fine sand Clay Fine sand Clay
12	Akwa Poly P3	7.6708	5.1556	4	377.0 31.8 265.7 45.0	0.8 8.6 57.9	0.8 9.4 67.3	Sandy clay Clay Sandy clay Clay
13	Ikot Ekpene Housing, Ifuho	7.6914	5.1832	3	441.5 1848.3 2405.8	3.6 63.4	3.6 67.0	Fine sand Coarse sand Gravelly sand
14	Ifuho	7.6900	5.1831	3	473.4 79.4 445.7	2.0 52.3	2.0 54.3	Fine sand Clay Fine sand
15	Ifuho	7.6844	5.1827	3	170.7 925.1 1959.4	1.7 68.1	1.7 69.8	Sandy clay Fine sand Gravelly sand
16	Ibong Ikot Akan	7.6775	5.1866	3	228.5 2111.6 434.5	6.1 49.3	6.1 55.4	Sandy clay Gravelly sand Fine sand

DOI: https://doi.org/10.48001/veethika.2024.10.02.003

VES No	Location	Longitude (Degrees)	Latitude (Degrees)	No. of Layers	Resistivity (Ωm)	Thickness (m)	Depth (m)	Lithology
17	Ibong Road	7.6792	5.1908	4	431.9 40.6 375.5 75.6	1.4 14.6 47.5	1.4 16.0 63.5	Fine sand Clay Fine sand Clay
18	Umuahia Road	7.6992	5.2024	4	224.4 59.1 1264.5 324.9	2.1 8.4 59.9	2.1 10.5 70.4	Sandy clay Clay Coarse sand Sandy clay
19	Ikono Road	7.7117	5.1981	3	207.4 2648.1 1506.3	4.5 80.9	4.5 85.4	Sandy clay Gravelly sand Coarse sand
20	Progress Road	7.7069	5.1794	4	157.3 66.8 1196.1 379.0	1.4 7.6 75.7	1.4 9.0 84.7	Sandy clay Clay Coarse sand Sandy clay

The depth to the water table was determined using the VES interpretation results and varies between 9.0 and 86.6 meters (Fig. 4a). There is an inverse relationship between the depth of the water table and the susceptibility of groundwater to surface contaminants. This means that as the water table gets deeper, groundwater becomes less vulnerable to surface contaminants, and vice versa. This relationship has been seen in studies conducted by Amiri et al. (2020) and George (2021). The depth rating ranges from 3 to 10, as seen in Figure 4b. The majority of the study region has a depth rating greater than 5, indicating a significant susceptibility to groundwater pollution or contamination from surface sources. The picture map in Figure 4 indicates that the areas with the largest exposure to groundwater are located around Umuahia Road, Progress Road, Ikpon Road, Utu Ikpe community, and Akwapoly. Net recharge (R) refers to the combined volume of water from rainfall and other human-made sources that is able to seep into the water table. The process of net recharge is the primary pathway for surface contaminants to enter the aquifer and contaminate groundwater. As a result, it is directly associated with the vulnerability rating (Abdullahi, 2009; Shirazi et al., 2013). Precipitation is the primary means by which groundwater is replenished in the study area. Since there was no available net recharge data in the area, the net recharge value was calculated using the equation (3) proposed by Piscopo (2001).

$$\text{Recharge value} = SF + RF + \text{SPF} \quad (3)$$

where SF is the slope factor, RF is the rainfall factor (mm) and SPF is the soil permeability factor.

Table 4 Summary of aquifer properties for the sounding locations

VES No	Location	Longitude (Degrees)	Latitude (Degrees)	Aquifer layer	Resistivity (Ωm)	Thickness (m)	Water table (m)	Lithology
1	Utu Ikpe 1	7.7038	5.1644	3	1750.8	49.2	11.1	Gravelly sand
2	Utu Ikpe 2	7.7031	5.1656	3	1621.6	–	62.3	Gravelly sand
3	Utu Ikpe 3	7.7053	5.1631	3	851.2	–	61.5	Gravelly sand
4	Utu Ikpe near Palace	7.7078	5.1598	3	2839.0	45.6	24.7	Gravelly sand
5	Abiakpo Edem Idim	7.7033	5.1491	3	2129.4	54.0	11.0	Gravelly sand
6	Ibiakpan Nto Akan	7.7400	5.1615	3	1341.6	–	66.0	Coarse sand
7	Utu Uyo Road	7.7442	5.1568	3	1097.0	–	63.1	Coarse sand
8	Ikpon Road	7.7292	5.1767	3	2478.6	61.4	12.4	Gravelly sand
9	Abiakpo Ntak Inyang	7.6667	5.1652	3	2632.2	–	55.6	Gravelly sand
10	Akwa Poly 1	7.6672	5.1588	3	214.4	–	86.6	Sandy clay
11	Akwa Poly 2	7.6706	5.1539	3	722.9	45.2	22.2	Fine sand
12	Akwa Poly 3	7.6708	5.1556	3	265.7	57.9	9.4	Sandy clay
13	Ikot Ekpene Housing, Ifuho	7.6914	5.1832	3	2405.8	–	67.0	Gravelly sand

DOI: https://doi.org/10.48001/veethika.2024.10.02.003

VES No	Location	Longitude (Degrees)	Latitude (Degrees)	Aquifer layer	Resistivity (Ωm)	Thickness (m)	Water table (m)	Lithology
14	Ifuho 1	7.6900	5.1831	3	445.7	–	54.3	Fine sand
15	Ifuho 2	7.6844	5.1827	3	1959.4	–	69.8	Gravelly sand
16	Ibong Ikot Akan	7.6775	5.1866	3	434.5	–	55.4	Fine sand
17	Ibong Road	7.6792	5.1908	3	375.5	47.5	16.0	Fine sand
18	Umuahia Road	7.6992	5.2024	3	1264.5	59.9	10.5	Coarse sand
19	Ikono Road	7.7117	5.1981	3	1506.3	–	85.4	Coarse sand
20	Progress Road	7.7069	5.1794	3	1196.1	75.7	9.0	Coarse sand

Table 5 Net Recharge ratings for the study (Piscopo, 2001; Al-Adamat et al. 2003)

Slope (%)	Rating	Rainfall (mm)	Rating	Soil permeability	Rating	Net recharge (weight $W=4$)	Rating
< 2	4	< 500	1	Very slow	1	11–13	10
2–10	3	500–700	2	Slow	2	9–11	8
10–33	2	700–850	3	Moderate	3	7–9	5
> 33	1	> 850	4	Mod–high	4	5–7	3
				High	5	3–5	1

The mean annual precipitation in the study region is approximately 2007.9 millimetres, as reported by Isaiah et al. in 2021. The percentage slope in the research area was derived using the ASTER digital elevation model (DEM) using ArcGIS 10.5. The digital elevation model (DEM) and slope values are provided in Figure 5a and 5b, respectively. In this work, the soil hydraulic conductivity (K) was determined using the empirical formula developed by Ekanem et al. (2020) for the specific area defined by Equation (4).

$$K = 139.12\rho_b^{-0.728} \quad (4)$$

where ρb represents the bulk resistivity of the soil layer. The soil permeability, Kp, was determined by calculating the soil hydraulic conductivity using the equation 5.

$$K_p = \frac{K\mu_d}{\delta_w g} \quad (5)$$

where δ_w is water density (1000 kg/m^3), g is acceleration due to gravity (9.8 m/s^2) and μ_d is the dynamic viscosity of water, which was taken as 0.0014 kg/ms (Fetter, 1994).

The calculated values of Kp vary from 1276.1 to 5865.2 millidarcies (mD). The slope, average annual rainfall, and soil permeability variables were evaluated based on the data provided in Table 5. The rainfall component was assigned a constant value rating of 4, whilst the slope and soil permeability factors were graded on a scale of 1 to 4, as shown in Figure 6. The ratings were arranged according to Equation (3) to calculate the net recharge values for each of the sounding stations, which range from 6 to 11 (Figure 7a). Figure 7 demonstrates that the southern region of the research area, specifically near Utu Ikpe village (Fig. 7a), experiences comparatively lower net recharge. This observation aligns with the findings from Fig. 6, which suggest that this area has the lowest slope and soil permeability ratings. The net recharge values were subsequently classed according to the data provided in Table 5. The net recharge values in the study region are rated on a scale of 3 to 10, as shown in Figure 7b. The lowest grade of 3–4 is found in the southern region of the study area. Figure 8a and 8b display the image maps of the DRASTIC depth and net recharge indices, which were generated by multiplying their respective ratings and weights. The depth index is lowest in certain areas in the northern region and near Akwapoly in the southwestern section of the research area. Similarly, the net recharge index is lowest in the southern region and also near Akwapoly in the Ikot Osurua village.

Aquifer media refers to the geological components that make up the aquifer. The permeability of the aquifer media, as indicated by the size of the grains in the aquifer materials (Ekanem et al., 2021), governs the reduction of contaminants (Amiri et al., 2020; Venkatesan et al., 2019). Aquifer geomaterials with higher permeability will have a reduced ability to remove contaminants, making them more vulnerable to contamination (Neh et al., 2015; Jaseela et al., 2016; Venkatesan et al., 2019; Amiri et al., 2020). The aquifer media used in this investigation were

DOI: https://doi.org/10.48001/veethika.2024.10.02.003

generated from the interpretation of VES data, which was limited by the geological borehole lithological logs. The aquifer consists of a mixture of fine and coarse sands, sandy clay in some areas, and gravelly sands in others. Table 1 awarded a fixed value of 3 to the sandy clay aquifer material and a fixed grade of 8 to the sands and gravel. The aquifer media has a weighted of 3, as indicated in Table 1. The picture map in Figure 9a displays the aquifer media index within the research area, which varies between 9 and 24. The whole research region exhibits a high aquifer media index, above 13, with the exception of a tiny section near Akwapoly.

Soil media refers to the uppermost layer of weathered material. The Earth's surface, where there is ongoing bioturbation. The composition of soil has a significant impact on the amount of rainfall that is able to seep down to the water table and the movement of pollutants (Jaseela et al., 2016; Amiri et al., 2020; George, 2021). The soils consist of a mixture of gravel, sand, and gravelly material.

Sands have high permeability, making any underlying hydrogeological units more vulnerable to contamination. The soil media were obtained from the borehole lithologically limited VES data interpretation results, similar to the aquifer media. The soil composition consists primarily of sand, including both fine and coarse sands, with occasional areas of sandy clay.

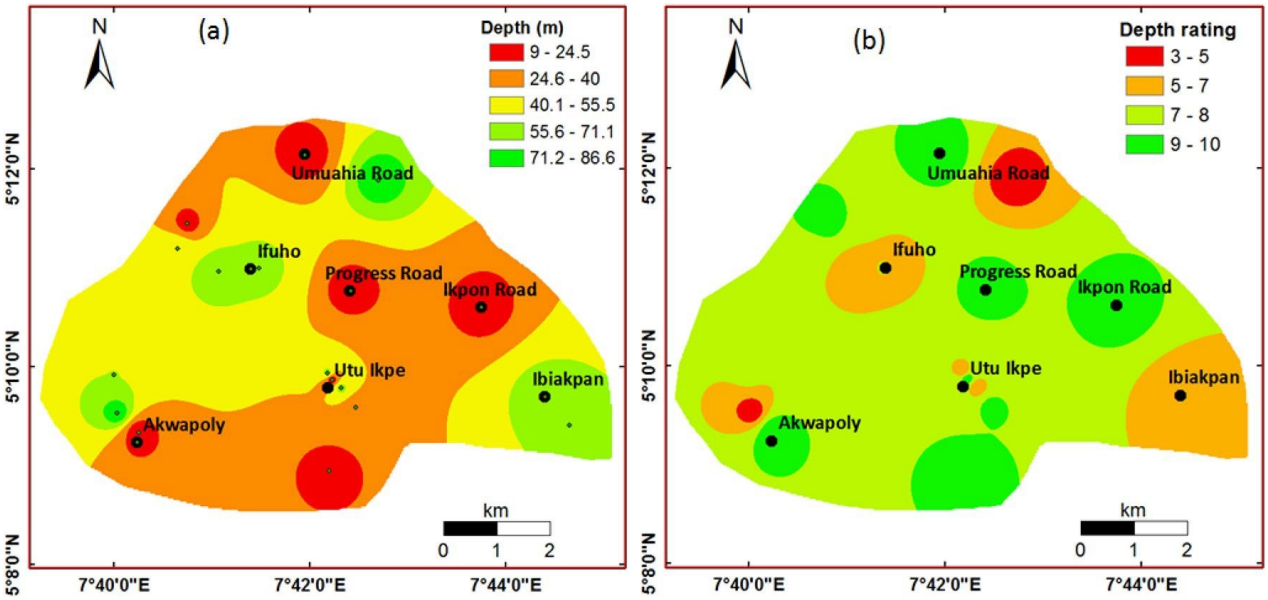

Figure 4: Distribution of depth to water table (**a**) and depth rating (**b**) in the study area

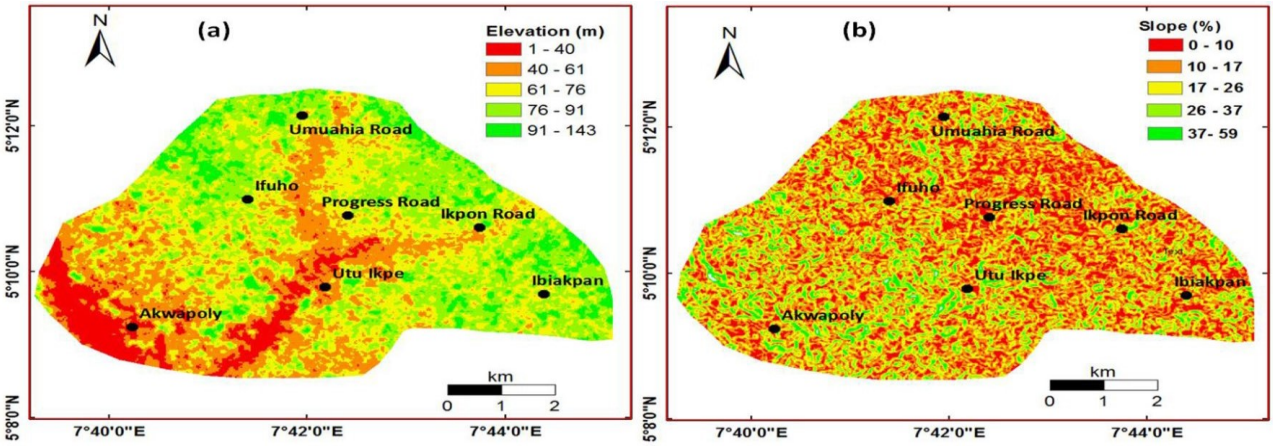

Figure 5: Topography of the study area **a** ASTER digital elevation model (DEM), **b** slope (%) in the study area

DOI: https://doi.org/10.48001/veethika.2024.10.02.003

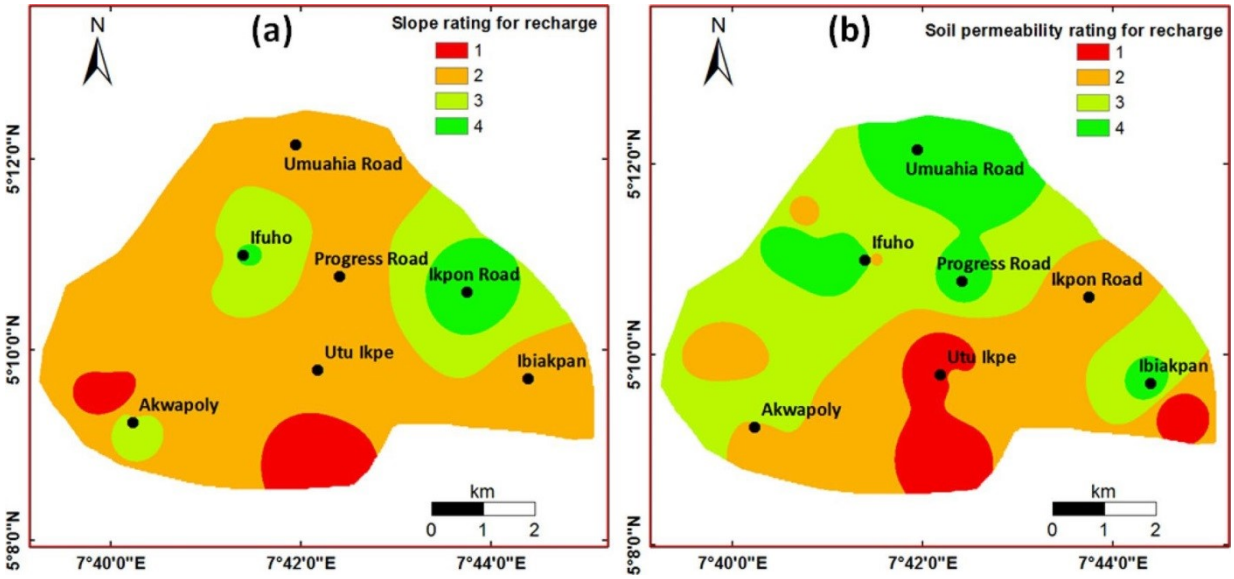

Figure 6: Net recharge estimation: **a** slope rating, **b** soil permeability rating

According to Table 1, the sandy clay soil was given a rating of 3, while the fine/coarse sands were given a grade of 9 for this characteristic. Figure 9b displays the soil media index in the research area, ranging from 6 to 18. Approximately 70% of the research region is characterized by a high soil media index, which is larger than 9. There are also dispersed pockets of low index, ranging from 6 to 9, as depicted in Figure 9b. Topography refers to the inclination or gradient of the Earth's surface. In places with a low slope, runoff water, also known as rainwater, will either stay in place or move at a very sluggish pace. This slow movement allows toxins to seep into the water table. As a result, locations with gentler inclines are more prone to contamination, depending on the characteristics of the soil. The slope gradient in the research region was derived using the ASTER digital elevation model (DEM) using ArcGIS 10.5. The slope gradient was then categorized into ratings ranging from 1 to 10, as specified in Table 1. Figure 10a displays the image map of the Topography index in the designated study area. Figure 10a illustrates that the region is marked by elevated levels

The topography index ranges from 4 to 10, with the exception of a small section in the south that has lower indices. The consequence of this is a reduced rate of runoff water in much of the research region, which will facilitate the infiltration of pollutants into the water table, resulting in a high vulnerability of groundwater. The vadose zone's influence the vadose zone is the stratum above the water table that is not saturated with water. This area is very important in the infiltration of precipitation into the aquifer layer (Aller et al., 1987). If the vadose zone consists of pervious or porous materials like sands and gravels, it can have a significant effect on the flow of polluted fluid.

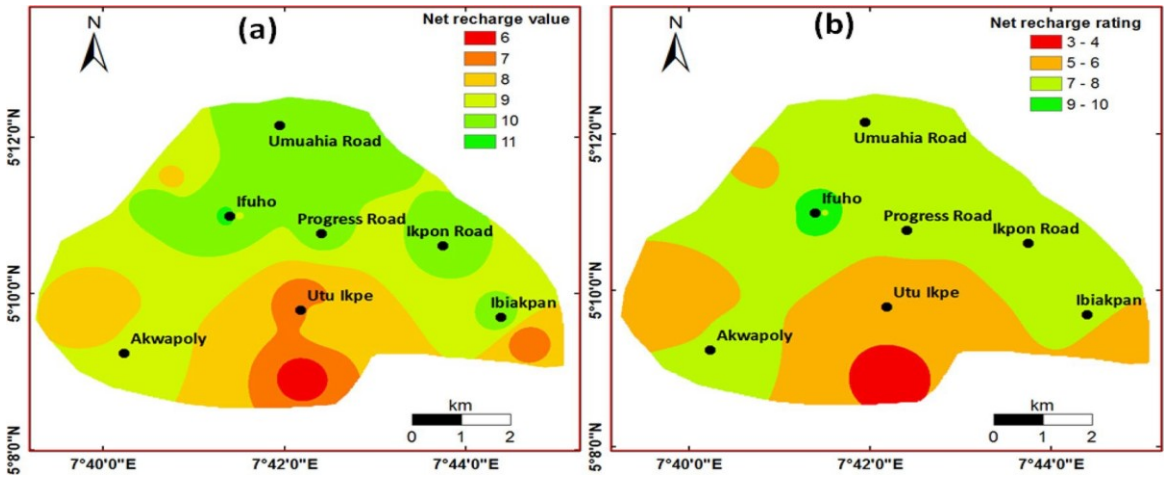

Figure 7: Distribution of net recharge: **a** values, **b** ratings in the study area

DOI: https://doi.org/10.48001/veethika.2024.10.02.003

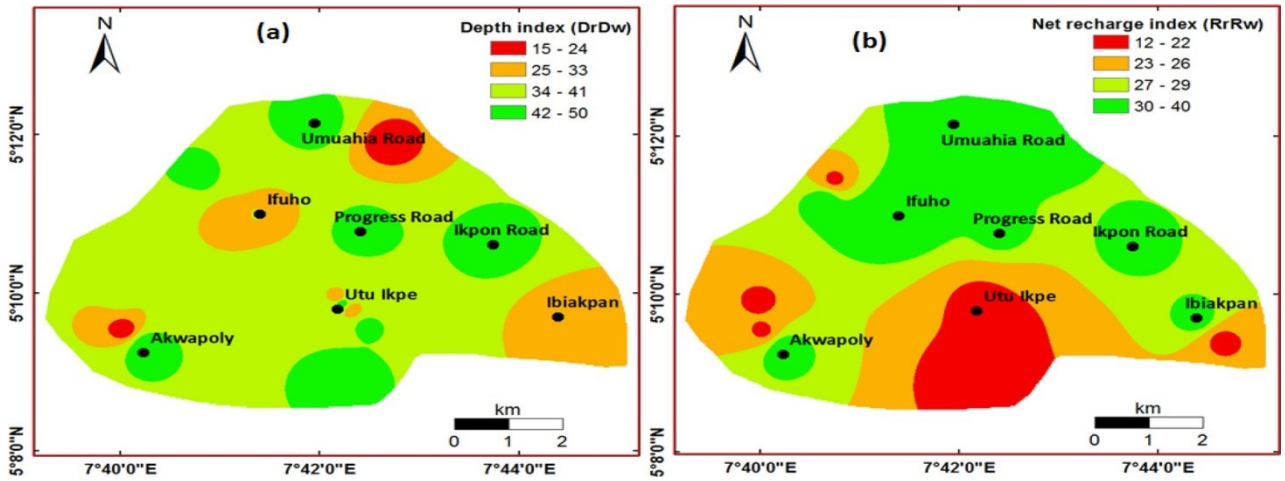

Figure 8: Image maps of **a** Depth index, **b** net recharge index in the study area

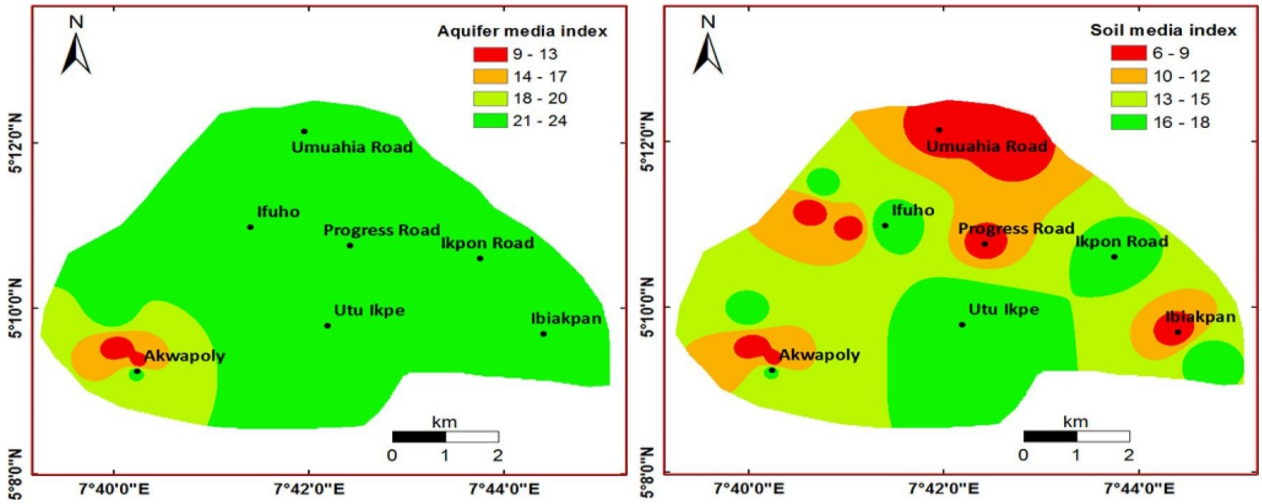

Figure 9: Image maps of **a** Aquifer media index, **b** Soil media index in the study area

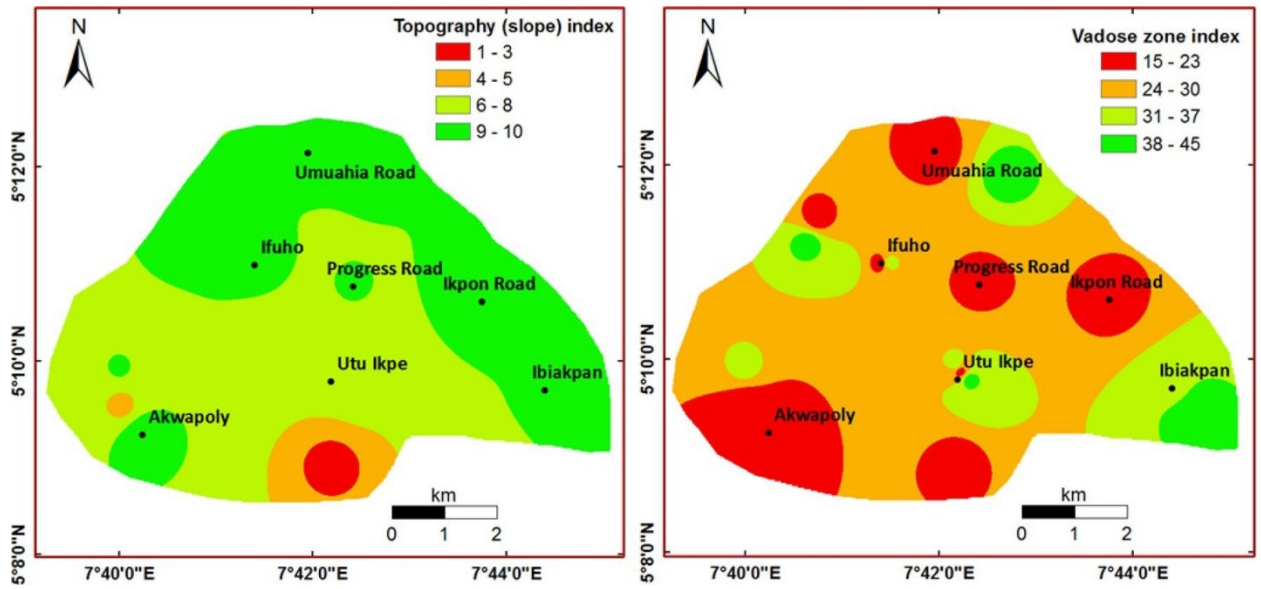

Figure 10: Image maps of **a** Topography index, **b** Vadose zone index in the study area

DOI: https://doi.org/10.48001/veethika.2024.10.02.003

The geomaterials of the vadose zone in this study were determined by the geological borehole lithologically constrained VES interpretation. These materials consist primarily of several types of sand (fine, coarse, and gravelly) as well as sandy clay. According to Table 1, this characteristic was given ratings of 3 for sandy clay, 7 for fine/coarse sands, and 9 for gravelly sands. The parameter has a weight of 5, as seen in Table 1. The vadose zone index in the study area varies from 15 to 45, as depicted in the image map of Fig. 10(b). This suggests that the study area is extremely susceptible to surface contamination. The majority of communities in the area have indexes ranging from 24 to 30. There are also some areas with very high indexes ranging from 31 to 45, as well as other areas with relatively low indexes ranging from 15 to 23. This distribution is shown in Figure 10b.

Significantly elevated indexes indicate a proportionally substantial influx of pollutants into the water table, resulting in a heightened susceptibility of the groundwater. Hydraulic conductivity refers to the ability of a material to transmit water or other fluids through it. This attribute is crucial as it directly influences the rate at which groundwater and pollutants move through an aquifer. The estimation in this investigation was conducted using Equation (4) and yielded a range of values from 4.9 × 10–6 to 3.2 × 10–5 m/s. The hydraulic conductivity range mentioned aligns with the values reported by Shamsuddin et al. (2018), George et al. (2021), and George (2021) for aquifers composed of fine to gravelly sand. The parameter has a weight of 3 and its values were assigned ratings ranging from 1 to 6, as indicated in Table 1. The hydraulic system exhibits significant fluctuation.

The significant fluctuation in hydraulic conductivity suggests a substantial variation in the grain size of the geomaterial components within the aquifer units in the region (Ekanem, 2022; Ikpe et al., 2022). The hydraulic conductivity index ranges from 3 to 18 in the studied area. Fig. 11a displays the distribution of these indexes. In certain areas of the northwestern and southwestern regions of the study area, low indexes ranging from 1 to 7 are seen, whereas the rest of the area is characterized by high indexes ranging from 8 to 18. These regions characterized by high indices are correlated with elevated susceptibility to groundwater contamination. The DRASTIC index (DI) and Groundwater vulnerability rating (GVR) were calculated by summing up the seven components stated earlier, using Eq. 2. The resulting DRASTIC index values for each sounding location are given in Table 6. The index ranges from 91 to 211, and its distribution in the research area is illustrated in Figure 11b. The final map indicating the vulnerability of groundwater was created by combining the seven parameters of the DRASTIC model for all the VES locations using ArcGIS 10.5 software. The resulting map can be shown in Figures 12 and 13. The values of the DRASTIC index were reassigned according to the information in Table 2 in order to establish three distinct categories for vulnerability evaluation. The classes are categorized as low (DI = 91), intermediate (DI = 149–172), and high (DI = 182–211) according to the information presented in Figure 12a and 12b. The analysis of the GVR results indicates that around 75% of the study region exhibits a high GVR, while around 20% displays a moderate GVR. The remaining 5% of the study area demonstrates a low GVR, as shown in Figure 12b. The predominant presence of moderate/high sensitivity zones in the area can be due to the combination of lower slope terrains and the high permeability of the sand layers in the aquifer. This allows contaminants to quickly infiltrate into the groundwater.

3.2 An examination of the sensitivity of the DRASTIC model.

A sensitivity study was conducted on the DRASTIC model outcomes to assess the impact of the ratings and weights provided to each input parameter on the final model results. It was crucial to do this because there was subjectivity involved in assigning ratings and weights to the input parameters of the model (Gogu & Dassargues, 2000b; Chitsazan and Akhtari, 2008). The analysis was conducted using two methodologies. The two approaches are the single parameter removal and the map removal approaches, respectively. The single parameter elimination approach assesses the impact of each input parameter on the final vulnerability index (Napolitano & Fabbri, 1996). The approach involves comparing the theoretical assigned weights with the effective weights W (expressed as a percentage) calculated using Equation (6) (Napolitano & Fabbri, 1996).

$$W = \frac{(P_r \times P_w)}{V} \times 100 \tag{6}$$

where P_r is the rating value, P_w is the theoretical assigned weight and V is the unperturbed vulnerability index.

The map removal sensitivity study, as described by Lodwick et al. (1990) and Napolitano & Fabbri (1996), examines the impact of eliminating individual parameters or groups of parameters on the resulting vulnerability index. The variation index, expressed as a percentage, quantifies the extent of variation resulting from the removal of one or more parameters. It was calculated using Equation (7) as described by Napolitano and Fabbri (1996).

DOI: https://doi.org/10.48001/veethika.2024.10.02.003

$$VI_i = \frac{(V - V_i)}{V} \times 100 \quad (7)$$

where VI_i is the variation index due to removal of parameters i and V_i is the perturbed vulnerability indices after the removal of parameter i. Both approaches have been successfully applied in the sensitivity analysis of DRASTIC model (Amiri et al., 2020; Gogu & Dassargues, 2000b; Khakhar et al., 2017).

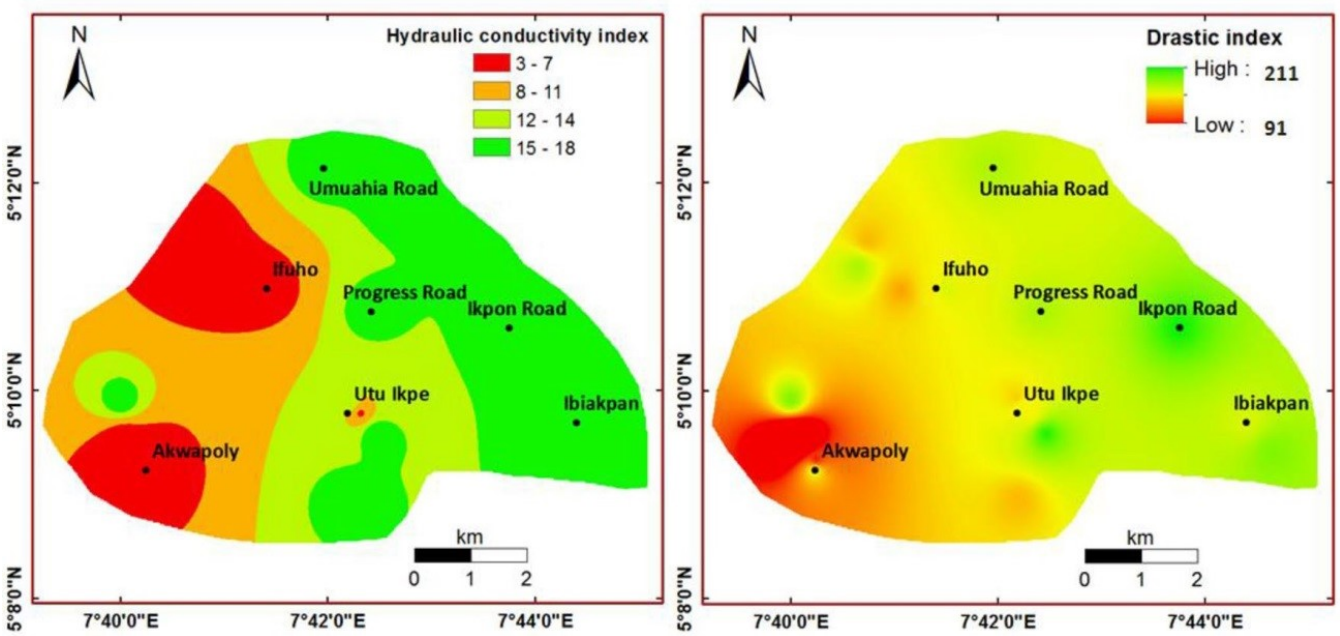

Figure 11: Image maps of **a** Hydraulic conductivity index, **b** DRASTIC index in the study area

VES No	Parameter	D		R		A		S		T		I		C		DI	GVR
	Weight	5		4		3		2		1		5		3			
	VES Location	D_r	D_rD_W	R_r	R_rR_W	A_r	A_rA_W	S_r	S_rS_W	T_r	T_rT_W	I_r	I_rI_W	C_r	C_rC_W		
1	Utu Ikpe 1	10	50	5	20	8	24	9	18	6	6	3	15	4	12	180	High
2	Utu Ikpe 2	5	25	5	20	8	24	9	18	6	6	7	35	4	12	179	High
3	Utu Ikpe 3	5	25	5	20	8	24	9	18	6	6	9	45	2	6	183	High
4	Utu Ikpe 4	9	45	5	20	8	24	9	18	6	6	7	35	6	18	207	High
5	Abiakpo Edem Idim	10	50	3	12	8	24	9	18	1	1	3	15	6	18	168	Moderate
6	Ibiakpan Nto Akan	5	25	8	32	8	24	3	6	8	8	7	35	6	18	188	High
7	Utu Uyo Road	5	25	5	20	8	24	9	18	8	8	9	45	6	18	203	High
8	Ikpon Road	10	50	8	32	8	24	9	18	10	10	3	15	6	18	211	High
9	Abiakpo Ntak Inyang	7	35	5	20	8	24	9	18	8	8	7	35	6	18	201	High
10	Akwa Poly P1	3	15	5	20	3	9	3	6	4	4	3	15	1	3	91	low
11	Akwa Poly P2	9	45	8	32	8	24	9	18	10	10	3	15	1	3	186	High
12	Akwa Poly P3	10	50	8	32	3	9	3	6	8	8	3	15	1	3	149	Moderate
13	Housing Ifuho	5	25	8	32	8	24	9	18	8	8	7	35	2	6	190	High
14	Ifuho 1	7	35	10	40	8	24	9	18	8	8	3	15	1	3	182	High
15	Ifuho 2	5	25	8	32	8	24	3	6	8	8	7	35	2	6	172	Moderate
16	Ibong Ikot Akan	7	35	8	32	8	24	3	6	8	8	9	45	1	3	190	High
17	Ibong Road	10	50	5	20	8	24	9	18	8	8	3	15	1	3	172	Moderate
18	Umuahia Road	10	50	8	32	8	24	3	6	8	8	3	15	6	18	189	High
19	Ikono Road	3	15	8	32	8	24	3	6	8	8	9	45	6	18	190	High
20	Progress Road	10	50	8	32	8	24	3	6	8	8	3	15	6	18	189	High

Table 6 Calculated DRASTIC index (DI) and groundwater vulnerability rating (GVR) in the study area

DOI: https://doi.org/10.48001/veethika.2024.10.02.003

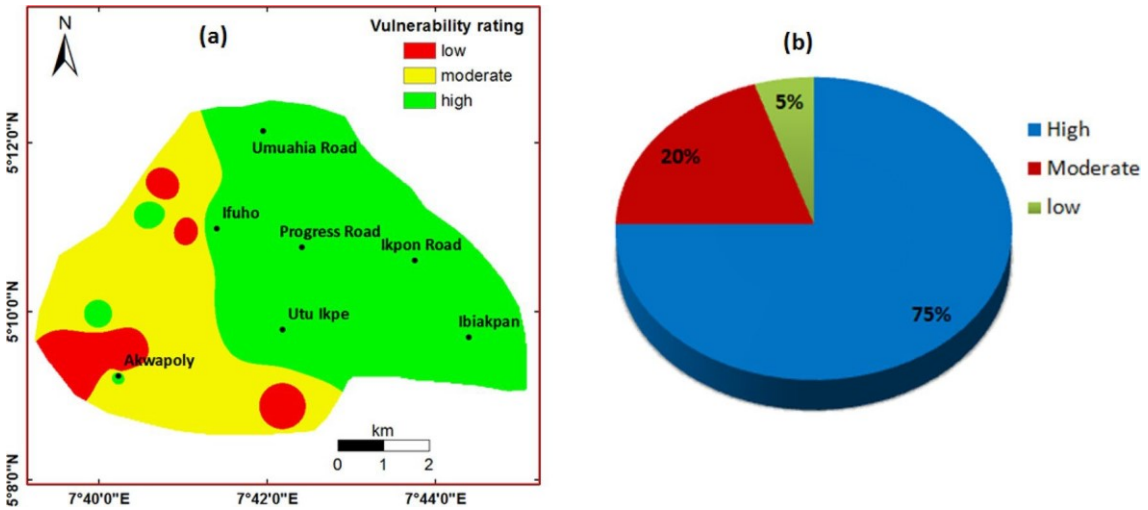

Figure 12: Groundwater vulnerability assessment result in the study area **a** Vulnerability rating map, **b** Percentages of the three classes of vulnerability rating

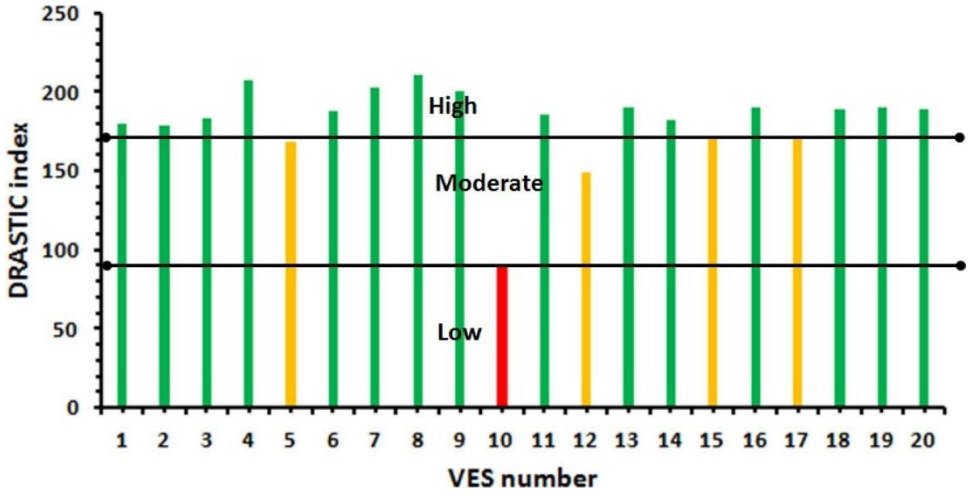

Figure 13: Bar chart showing the groundwater vulnerability ratings (GWR) of the VES stations in the study area

Table 7 Statistical summary of the DRASTIC parameters

	D	*R*	*A*	*S*	*T*	*I*	*C*
Minimum	3.0	3.0	3.0	3.0	1.0	3.0	1.0
Maximum	10.0	10.0	8.0	9.0	10.0	9.0	6.0
Mean	7.3	6.7	7.5	6.6	7.3	5.4	3.7
standard deviation	2.6	1.8	1.5	3.0	2.0	2.6	2.3
Coefficient of variation	35.5	27.7	20.5	45.7	27.9	47.5	62.1

DOI: https://doi.org/10.48001/veethika.2024.10.02.003

Table 7 displays the statistical summary of the DRASTIC parameters utilized in calculating the ultimate DRASTIC index. The mean values quantify the level of contamination risk associated with each of the criteria. The aquifer medium presents the greatest risk of groundwater contamination, with an average value of 7.5. Next in the sequence are the measurements for the depth to the water table and the topography, both having an average value of 7.3. This is followed by the recharge parameter, which has an average value of 6.7. The soil media has an average value of 6.6, while the impact of the vadose zone has an average value of 5.4. Finally, the aquifer hydraulic conductivity has an average value of 3.7.

The coefficient of variation (CV in %) quantifies the impact of each parameter on the overall variation of the vulnerability index. According to Table 8, the aquifer hydraulic conductivity has the greatest impact on the fluctuation in the vulnerability index, with a coefficient of variation (CV) of 62.1%. The aquifer media has the lowest degree of fluctuation, with a coefficient of variation (CV) of 20.5%. The findings of the single parameter removal sensitivity analysis are displayed in Table 8. All parameters have variation index values larger than one, indicating that removing a parameter will decrease the vulnerability index. In this particular situation, the parameter that was eliminated has a greater impact on the calculated vulnerability index. According to Table 8, the greatest amount of variation is observed when the depth to the water table is eliminated, with an average difference of 20.2%. This is followed by the net recharge, which has an average variation of 18.7%. One likely reason for this is the elevated theoretical weights of 5 and 4, along with the elevated ratings of 3 to 10 attributed to these parameters, respectively. The vulnerability varies depending on the removal of the vadose zone, aquifer media, soil media, and aquifer hydraulic conductivity, as seen in Table 8. The smallest amount of variation occurs when the aquifer hydraulic conductivity parameter is excluded, with an average variation of 7.9%. This is likely because this parameter has a weight of 3 and is rated between 1 and 6. Table 9 displays the changes in the vulnerability index resulting from the elimination of one or multiple input parameters. The removal of the characteristics was carried out in ascending order of their influence on the final vulnerability index, as indicated by the findings presented in Table 8. The results shown in Table 9 are comparable to those in Table 8, indicating that depth, net recharge, and vadose zone have a greater impact on the vulnerability index than soil medium, slope, and aquifer hydraulic conductivity parameters.

Table 8 Statistics of single parameter removal sensitivity analysis

Parameters Removed	Mean Variation Index (%)
D (depth)	20.2
R (recharge	18.7
A (aquifer media)	16.5
S (soil media)	10.9
T (topography)	8.0
I (impact of vadose zone)	17.8
C (aquifer hydraulic conductivity)	7.9

Table 9 Statistics of map removal sensitivity analysis

	(%)
Parameters used	Mean variation index
DRASTI	7.9
DRASI	16.0
DRAI	28.9
DRI	43.3
DR	61.1
D	79.8

The average data indicate that the vulnerability index fluctuation rises as additional input factors are eliminated. This phenomenon could be attributed to the theoretical weights provided to the different factors, the relatively less robust representation of the layers compared to the site circumstances, and the inherent fluctuations of the individual parameter within the research region (Khakhar et al., 2017). Reducing the number of input parameters in the DRASTIC model leads to greater fluctuations in the final vulnerability index, which aligns with the findings of Khakhar et al. (2017). This demonstrates that all the DRASTIC factors are crucial in calculating the vulnerability index. Table 10 displays the outcomes of the single parameter sensitivity analysis. The findings indicate that depth, net recharge, vadose zone, and aquifer media are the primary factors in determining the final vulnerability score in this study. This is also consistent with the findings of the map removal sensitivity analysis.

DOI: https://doi.org/10.48001/veethika.2024.10.02.003

Table 10 Statistics of single parameter sensitivity analysis

Parameter	Theoretical	Theoretical	Effective weight (%)			
	weight	weight (%)	Mean	Minimum	Maximum	Sd
D	5	21.7	25.3	8.3	48.1	11.1
R	4	17.4	18.2	9.8	30.8	5.7
A	3	13.0	15.0	8.7	19.5	2.5
S	2	8.7	8.9	3.3	14.6	3.9
T	1	4.3	4.9	0.8	7.7	1.4
I	5	21.7	17.6	9.0	28.1	6.5
C	3	13.0	7.2	1.9	14.6	4.3

4. CONCLUSION

This study utilized the DRASTIC model and GIS tools to evaluate the susceptibility of groundwater in the Ikot Ekpene municipality and surrounding areas in southern Nigeria. A total of twenty vertical electrical soundings were conducted at specific places within the study region. The geological borehole lithologically limited VES data interpretation reveals that the research area consists of three to four distinct layers composed of sand (fine, coarse), gravel, and sandy clay.

The third layer is the hydrogeological unit in the area that can be commercially exploited. It is located at a depth ranging from 9.0 to 86.6 meters. These findings align with the outcomes of George et al. (2014) and Ikpe et al. (2022) who employed a similar methodology to examine the surface characteristics in the region. The DRASTIC model utilized seven environmental parameters: depth to the water table, net recharge, aquifer medium, topography, impact of vadose zone, and hydraulic conductivity. All parameters, with the exception of topography, were derived based on the results of VES data interpretation. This approach offers the benefits of cost-effectiveness and environmental friendliness, as the required parameters may be quickly collected from surface measurements without the need for drilling any boreholes (Ekanem et al., 2020; George et al., 2014, 2017, 2018; Ikpe et al., 2022; Thomas et al., 2020). The topography was derived from the ASTER digital elevation model (DEM) using ArcGIS 10.5. The quantile classification of the ArcGIS 10.5 reveals that approximately 75% of the research area is categorized as high GVR zone, around 20% is classified as moderate GVR zone, and the remaining 5% is classified as low GVR zone. The greater proportion of the region deemed to have moderate/high groundwater vulnerability rating (GVR) may be attributed to the presence of predominantly low-gradient terrains, characterized by high permeable sandy shallow layers situated above the water table. As a result, this specific area of the research experiences effortless and swift penetration of surface pollutants into the groundwater because there are no sufficient impermeable layers to protect it. The statistical analysis of the DRAS-TIC index values indicates that the aquifer media presents the highest level of risk for groundwater contamination, followed by the depth to water table and topography. The aquifer hydraulic conductivity poses the least amount of risk, as it has been demonstrated to have the greatest impact on the final computed DRASTIC index. The aquifer media has the smallest impact on the final index. The findings of the sensitivity analysis, specifically the single parameter removal and map removal, suggest that the final DRASTIC index is very sensitive to all the parameters. Among these parameters, depth, net recharge, vadose zone, and aquifer media are found to be the most relevant. Regions characterized by a high DRASTIC index indicate a significant susceptibility to possible harm, and the aquifers in these regions have inadequate protection against contaminants that are present on or near the surface.

75% of the research area has been delineated as high groundwater susceptibility zones on the vulnerability rating map. The delineated zones closely align with the zones described by Ikpe et al. (2022) as having inadequate protection for the aquifer. The aquifers in these designated areas lack sufficient safeguards against pollutants that are present on or near the surface. As a result, the water quality from boreholes sunk in these areas cannot be assured, which presents a significant threat to human health and ecological services in the region. The hazard assessment map undoubtedly offers valuable information that might assist managers, local government planners, and supervisory authorities like the Akwa Ibom State water corporation in determining the optimal locations for boreholes in the region. The Akwa Ibom state environmental agency should prioritize the establishment of adequate drainage and sewer infrastructure in the study

DOI: https://doi.org/10.48001/veethika.2024.10.02.003

area to facilitate efficient waste management, potentially directing the garbage towards the ravine area, which is uninhabited and does not include water boreholes. An extensive waste management strategy should be implemented for the residents of the region to adhere to regarding the daily disposal of waste in order to protect the aquifers in the area, which are already susceptible to contamination. The local authorities should implement a regulation that strictly prohibits the disposal of solid garbage beside the road or street. While the groundwater vulnerability map is useful for identifying areas that are extremely susceptible to contamination, it cannot replace the need for on-site hydrogeological research.

REFERENCES

Abdullahi, U. (2009). Evaluation of models for assessing groundwater vulnerability to pollution in Nigeria. *Bayero Journal of Pure Applied Science, 2*, 138–142.

Abu-Bakr, H. A. (2020). Groundwater vulnerability assessment in different types of aquifers. *Agricultural Water Management, 240*(2020), 106275. https://doi.org/10.1016/j.agwat.2020.106275

Aller L, Bennett T, Lehr JH, Petty RJ, Hackett G (1987) DRASTIC: a standardised system for evaluating groundwater pollution potential using hydrogeologic settings. US-EPA Report 600/2-87-035

Amiri, F., Tabatabaie, T., & Entezari, M. (2020). GIS-based DRASTIC and modified DRASTIC techniques for assessing groundwater vulnerability to pollution in Torghabeh-Shandiz of Khorasan County Iran. *Arabian Journal of Geoscience, 13*, 479. https:// doi.org/10.1007/s12517-020-05445-0

Awawdeh, M. M., & Jaradat, R. A. (2010). Evaluation of aquifers vulnerability to contamination in the Yarmouk River basin, Jordan, based on DRASTIC method. *Arabian Journal of Geoscience, 3*(3), 273–282.

Awawdeh, M., Obeidat, M., & Zaiter, G. (2015). Groundwater vulnerability assessment in the vicinity of Ramtha wastewater treatment plant, North Jordan. *Applied Water Science, 5*, 321–334. https:// doi.org/10.1007/s13201-014-0194-6

Barbulescu, A. (2020). Assessing groundwater vulnerability: DRASTIC and DRASTIC-like methods: A review. *Water, 12*, 1356. https://doi.org/10.3390/w12051356

Barres-Lallemend A (1994) Normalization des criteres d'etablissement desrtes de ulnerabilite aux pollutions. Etude documentaire pre- liminaire. BRGM R3792

Bello, A. M. A., Makinde, V., & Coker, J. O. (2010). Geostatistical analyses of accuracies of geologic sections derived from interpreted vertical electrical soundings (VES) data: an examination based on VES and *Borehole Data Collected from the Northern Part of Kwara* State, Nigeria. *Journal of American Science, 6*(2), 24–31. (ISSN: 1545–1003).

Boufekane, A., & Saighi, O. (2013). Assessment of groundwater pollution by nitrates using intrinsic vulnerability methods: A case study of the Nile valley groundwater (Jijel, North-East Algeria). *African Journal of Environmental Science Technology, 7*(10), 949–960. https://doi.org/10.5897/AJEST2013.142

Civita M (1990) La valutacione della vulnerabilitia degli aquifer all'inquinamamento. In: Proceedings of 1st con. naz. protezione egestione delle aque sotterranee: metodologie, technologie e obi- ettivi, 20–22 September, Maranosul Panaro, pp. 39–86

Dobrin, M. B., & Savit, C. H. (1988). *Introduction to geophysical prospecting* (4th ed.). McGraw-Hill Book Company.

Doerfliger, N., Jeannin, P. Y., & Zwahlen, F. (1999). Water vulnerability assessment in karst environments: A new method of defining protection areas using a multi-attribute approach and GIS tools (EPIK method). *Environmental Geology, 39*, 165–176.

Edet, A. E., & Okereke, C. S. (2002). Delineation of shallow ground- water aquifers in the coastal plain sands of Calabar area (Southern Nigeria) using surface resistivity and hydrogeological data. *Journal of African Earth Sciences, 35*(3), 433–443.

Ekanem KR, George NJ, Ekanem AM (2022) Parametric characterization, protectivity and potentiality of shallow hydrogeological units of a medium-sized housing estate, Shelter Afrique, Akwa Ibom State, Southern Nigeria. *Acta Geophysica*

Ekanem, A. M. (2020). Georesistivity modelling and appraisal of soil water retention capacity in Akwa Ibom State University main campus and its environs Southern Nigeria. *Modelling Earth*

DOI: https://doi.org/10.48001/veethika.2024.10.02.003

System and Environment, 6, 2597–2608. https://doi.org/10.1007/ s40808-020-00850-6

Ekanem, A. M. (2021). Estimation of aquifer geohydrodynamic properties using the Inverse Slope method. *Researchers Journal of Science and Technology (REJOST), 1*, 1–16.

Ekanem, A. M. (2022). AVI- and GOD-based vulnerability assessment of aquifer units: A case study of parts of Akwa Ibom State, Southern Niger Delta, Nigeria. *Sustainable Water Resource Management, 8*, 29. https://doi.org/10.1007/s40899-022-00628-x

Ekanem, A. M., Akpan, A. E., George, N. J., & Thomas, J. E. (2021). Appraisal of protectivity and corrosivity of surficial hydrogeological units via geo-sounding measurements. *Environmental Monitoring and Assessment, 193*, 718. https://doi.org/10.1007/ s10661-021-09518-9

Ekanem, A. M., George, N. J., Thomas, J. E., & Nathaniel, E. U. (2020). Empirical Relations Between Aquifer Geohydraulic- Geoelectric Properties Derived from Surficial Resistivity Measurements in Parts of Akwa Ibom State, Southern Nigeria. *Natural Resources Research, 29*(4), 2635–2646. https://doi.org/ 10.1007/s11053-019-09606-1

Esu, E. O., Okereke, C. S., & Edet, A. E. (1999). A regional hydrostratigraphic study of Akwa Ibom State southeastern Nige- ria. *Global Journal of Pure and Applied Sciences, 5*(1), 89–96.

Fetter, C. W. (1994). *Applied hydrogeology* (3rd ed., p. 600). Prentice Hall Inc.

Foster SSD (1987) Fundamental concepts in aquifer vulnerability, pollution risk and protection strategy. In: Duijvenbooden W, Waegeningh HG (eds) vulnerability of soil and groundwater to pollutants. TNO Committee on Hydrological Research, The Hague, Proc Info 38, 69–86

Foster, S., Hirata, R., & Andreo, B. (2013). The aquifer pollution vulnerability concept: Aid or impediment in promoting ground- water protection? *Hydrogeology Journal, 21*(7), 1389–1392.

George, N. J. (2021). Geo-electrically and hydrogeologically derived vulnerability assessments of aquifer resources in the hinterland of parts of Akwa Ibom State, Nigeria. *Solid Earth Sciences, 6*(2), 70–79.

George, N. J., Akpan, A. E., & Ekanem, A. M. (2016a). Assessment of textural variational pattern and electrical conduction of economic and accessible Quaternary hydrolithofacies via geo- electric and laboratory methods in SE Nigeria: A case study of select locations in Akwa Ibom State. *Journal of the Geo- logical Society of India, 88*, 517–528. https://doi.org/10.1007/ s12594-016-0514-6

George, N. J., Bassey, N. E., Ekanem, A. M., & Thomas, J. E. (2020). Effects of anisotropic changes on the conductivity of sedimentary aquifers, southeastern Niger Delta, Nigeria. *Acta Geophysica., 68*, 1833–1843. https://doi.org/10.1007/ s11600-020-00502-4

George, N. J., Ekanem, A. M., Ibanga, J. I., & Udosen, N. I. (2017). Hydrodynamic Implications of Aquifer Quality Index (AQI) and Flow Zone Indicator (FZI) in groundwater abstraction: A case study of coastal hydro-lithofacies in South-eastern Nigeria. *Journal of Coastal Conservation, 21*, 759–776. https://doi.org/10. 1007/s11852-017-0535-3

George, N. J., Ekanem, A. M., Thomas, J. E., & Harry, T. A. (2021). Modelling the effect of geo-matrix conduction on the bulk and pore water resistivity in hydrogeological sedimentary beddings. *Modelling Earth Systems and Environment, 8*, 1335–1349. https:// doi.org/10.1007/s40808-021-01161-0

George, N. J., Ibuot, J. C., Ekanem, A. M., & George, A. M. (2018). Estimating the indices of inter-transmissibility magnitude of active surficial hydrogeologic units in Itu, Akwa Ibom State, southern Nigeria. *Arabian Journal of Geosciences, 11*, 134. https://doi.org/10.1007/s12517-018-3475-9

George, N. J., Ubom, A. I., & Ibanga, J. I. (2014). Integrated approach to investigate the effect of leachate on groundwater around the Ikot Ekpene Dumpsite in Akwa Ibom State, Southeastern Nigeria. *International Journal of Geophysics, 174589*, 1–12. https://doi. org/10.1155/2014/174589

Gogu, R. C., & Dassargues, A. (2000a). Current trends and future challenges in groundwater vulnerability assessment using over- lay and index methods. *Environmental Geology, 39*, 549–559.

Gogu, R. C., & Dassargues, A. (2000b). Sensitivity analysis for the EPIK method of vulnerability assessment in a small karstic aquifer, southern Belgium. *Hydrogeology Journal, 8*, 337–345. Harter T, Walker LG (2001) Assessing Vulnerability of Groundwater. pp. 9–17. 35.

DOI: https://doi.org/10.48001/veethika.2024.10.02.003

www.dhs.ca.gov/ps/ddwem/dwsap/DWSAPindex.htm

Ikpe, E. O., Ekanem, A. M., & George, N. J. (2022). Modelling and assessing the protectivity of hydrogeological units using primary and secondary geoelectric indices: A case study of Ikot Ekpene Urban and its environs, southern Nigeria. *Modelling Earth System and Environment*. https://doi.org/10.1007/ s40808-022-01366-x

Isaiah, A. I., Yamusa, A. M., & Odunze, A. C. (2021). Advanced Study on Variability in Length of Rainy Season for Selected Crops Production in Coastal and Upland Areas of Akwa Ibom State, Nigeria. *Cutting- Edge Research in Agricultural Sciences, 6*(5), 101–109. https://doi.org/10.9734/bpi/cras/v6/2424E

Jaseela, C., Prabhakar, K., Sadasivan, P., & Harikumar, H. P. (2016). Application of GIS and DRASTIC modelling for evaluation of groundwater vulnerability near a solid waste disposal site. *Inter- national Journal of Geosciences, 7*, 558–571. https://doi.org/10. 4236/ijg.2016.74043

Khakhar, M., Ruparelia, J. P., & Vyas, A. (2017). Assessing ground- water vulnerability using GIS-based DRASTIC model for Ahmedabad district, India. *Environmental Earth Science, 76*, 440. https://doi.org/10.1007/s12665-017-6761-z

Kumar, A., & Krishna, A. P. (2020). Groundwater vulnerability and contamination risk assessment using GIS-based modified *DRAS- TIC*-LU model in hard rock aquifer system in India. *Geocarto International, 35*(11), 1149–1178. https://doi.org/10.1080/10106049.2018.1557259

Li, P., Karunanidhi, D., Subramani, T., & Srinivasamoorthy, K. (2021). Sources and consequences of groundwater contamination. *Archives of Environmental Contamination and Toxicology, 80*, 1–10. https://doi.org/10.1007/s00244-020-00805-z

Lodwick, W. A., Monson, W., & Svoboda, L. (1990). Attribute error and sensitivity analysis of map operations in geographical information systems: suitability analysis. *International Journal of Geographical Information System, 4*(4), 413–428.

Machiwal, D., Jha, M. K., Singh, V. P., & Mohan, C. (2018). Assessment and mapping of groundwater vulnerability to pollution: Cur- rent status and challenges. *Earth-Science Reviews, 185*, 901–927.

Maxe, L., & Johansson, P.-O. (1998). Assessing groundwater vulnerability using travel time and specific surface area as indicators. *Hydrogeology Journal, 6*, 441–449.

Mbipom, E. W., Okwueze, E. E., & Onwuegbeche, A. A. A. (1996). Estimation of transmissivity using VES data from Mbaise area of Nigeria. *Nigerian Journal of Physics, 85*, 28–32.

Napolitano, P., & Fabbri, A. G. (1996). Single-parameter sensitivity analysis for aquifer vulnerability assessment using DRASTIC and SINTACS. HydroGIS 96 Application of Geographic Information Systems in Hydrology and Water Resources Management. *IAHS, 235*, 559–566.

Neh, A. V., Ako, A. A., Ayuk, A. R., & Hosono, T. (2015). DRASTIC - GIS model for assessing vulnerability to pollution of the phreatic aquiferous formations in Douala-Cameroon. *Journal of African Earth Sciences, 102*, 180–190. https://doi.org/10.1016/j. jafrearsci.2014.11.001

NRC (National Research Council). (1993). *Ground Water Vulnerability Assessment: Contamination Potential under Conditions of Uncertainty*. National Academy Press.

Obaje, NG (2009) Geology and Mineral Resources of Nigeria. London: Springer Dordrecht Heidelberg, Pp5–14.

Piscopo G (2001) Groundwater vulnerability map, explanatory notes, Castlereagh Catchment. Australia NSW Department of Land and Water Conservation, Parramatta. https://www.industry.nsw.gov. au/ data/assets/pdf_file/0004/151762/Castlereagh-map-notes. pdf . Accessed March 14th 2022.

Reijers, T. J. A., & Petters, S. W. (1987). Depositional environments and diagenesis of Albian Carbonates on the Calabar Flank, SE Nigeria. *Journal of Petroleum Geology, 10*(3), 283–294.

Shamsuddin, M. K. N., Sulaiman, W. N. A., Ramli, M. F., & Kusin, F. M. (2018). Vertical hydraulic conductivity of riverbank and hyporheic zone sediment at Muda River riverbank filtration site, Malaysia. *Applied Water Science*. https://doi.org/10.1007/ s13201-018-0880-x

DOI: https://doi.org/10.48001/veethika.2024.10.02.003

Shirazi, S. M., Imran, H. M., Akib, S., Yusop, Z., & Harun, Z. B. (2013). Groundwater vulnerability assessment in the Melaka State of Malaysia using DRASTIC and GIS techniques. *Environment and Earth Science, 70*, 2293–2304. https://doi.org/10.1007/ s12665-013-2360-9

Short, K. C., & Stauble, A. J. (1967). Outline Geology of the Niger Delta. *AAPG Bulletin, 51*, 761–779.

Stacher, P. (1995). Present Understanding of the Niger Delta hydrocar- bon habitat. In M. N. Oti & G. Postma (Eds.), *Geology of Deltas: Rotterdam* (pp. 257–267). Balkema.

Thomas, J. E., George, N. J., Ekanem, A. M., & Nsikak, E. E. (2020). Electrostratigraphy and hydrogeochemistry of hyporheic zone and water-bearing caches in the littoral shorefront of Akwa Ibom State University, Southern Nigeria. *Environmental Monitoring and Assessment, 192*, 505. https://doi.org/10.1007/ s10661-020-08436-6

Udoh, F. E., Nyakno, J. G., & Ekanem, A. M. (2015). Analysis of microstructural properties of Paleozoic aquifer in the Benin Formation, using Grain Size Distribution Data from Water Borehole in Akwa Ibom State, Nigeria. *IOSR Journal of Applied Geology and Geophysics, 3*(4), 25–30. https://doi.org/10.9790/0990-03422530

Umoh, S. D., & Etim, E. E. (2013). Determination Of Heavy Metal Contents From Dumpsites Within Ikot Ekpene, Akwa Ibom State, Nigeria Using Atomic Absorption Spectrophotometer. *The International Journal of Engineering and Science (IJES), 2*(2), 123–129.

United States Environmental Protection Agency (US EPA) (1994) Handbook: Groundwater and Wellhead Protection. US EPA Report No. EPA/625/R-94/001, Washington, DC, p 239

Van Stempvoort D, Ewert L, Was-senaar L (1992) AVI: A method for groundwater protection mapping in the prairie provinces of Canada. Prairie Provinces Water Board Report 114, Regina, SK

Venkatesan, G., Pitchaikani, S., & Saravanan, S. (2019). Assessment of groundwater vulnerability using GIS and DRASTIC for Upper Palar River Basin, Tamil Nadu. *Journal of the Geological Society of India, 94*, 387–394. https://doi.org/10.1007/s12594-019-1326-2

Vrba J, Zaporozec A (1994) Guidebook on Mapping Groundwater Vulnerability, Vol. 16. International Contribution to Hydrogeology, Hannover, 131 p.

Vrbka, P., Ojo, O. J., & Gebhardt, H. (1999). Hydraulic characteristics of Maastrichtian sedimentary rocks of the southeastern Bida Basin, central Nigeria. *Journal of African Earth Science, 29*(4), 659–667.

Zohdy AAR, Eaton GP, Mabey DR (1974) Application of surface geo- physics to groundwater investigation. USGS techniques of water resources investigations 02-D1. https://doi.org/10.3133/twri02D1

How to cite this Article:

Ikpe E. O., Inyang U U, Sampson E. A (2024), Utilizing Geological and Geoelectrical methods in a GIS-based DRASTIC model of the Probable Groundwater Vulnerability in the Southern Nigerian Raffia Metropolis of Ikot Ekpene and its Surroundings, VEETHIKA-An International Interdisciplinary Research Journal, 10(2), pp. 18-39. DOI: https://doi.org/10.48001/veethika.2024.10.02.003